Supporting Information for

Reaction Pathways of Proton Transfer in Hydrogen Bonded Phenol-Carboxylate Complexes Explored by UVNMR

Benjamin Koeppe,[1] Peter M. Tolstoy,[1,2*] Hans-Heinrich Limbach[1]

[1] Institute of Chemistry and Biochemistry, Freie Universität Berlin, Germany

[2] V.A. Fock Institute of Physics, St. Petersburg State University, Russia.

Sample composition as determined by ^{1}H NMR.

Table S1. Approximate relative composition of samples as determined by ^{1}H NMR.

		UVNMR samples (Type A) c(HA)≈ 1 mM			^{13}C NMR samples (Type B) c(HA)≈ 3 mM		
	HX	**n(HA)**	**n(X-)**	**n(HX)**	**n(HA)**	**n(X-)**	**n(HX)**
2	{N/A}	1	70	0			
4	hydrogen tetrafluoroborate	1	7	0	1	8	0
5	hydrogen iodide	1	10	0	1	3	0
6	hydrogen bromide	1	19	0	1	3	0
7	hydrogen chloride	1	7	0	1	2	0
8	trifluoroacetic acid	1	19	0	1	3	0
9	dichloroacetic acid	1	42	6	1	5	0
10	2,3,5-trichlorobenzoic acid	1	47	13	1	5	1
11	chloroacetic acid	1	25	10	1	1	0
12	3,5-dichlorobenzoic acid	1	14	12	1	4	1
13	formic acid	1	13	12	1	1	0
14	4-chlorobenzoic acid	1	10	9	1	1	0
15	benzoic acid	1	20	21	1	9	1
16	4-chlorophenylacetic acid	1	20	20	1	1	0
17	4-tert-butylbenzoic acid	1	15	16	1	3	1
18	phenylacetic acid	1	16	17	1	6	7
19	3-phenylpropionic acid	1	20	27	1	7	11
20	acetic acid	1	17	25	1	1	0
21	4-phenylbutyric acid	1	14	20	1	1	0
22	pivalic acid	1	10	12	1	2	0
23	2,4,5-trichlorophenol	1	20	24	1	1	0
25	2,4-dichlorophenol	1	19	30	1	10	17
26	4-chlorophenol	1	10	18	1	6	11
27	4-methylphenol	1	14	27	1	11	9

In Table S1 the letter **n** stands for the concentration of the corresponding moiety (normalised to the amount of chromophore) as calculated from the integrated intensity in NMR spectra.

Table S2. Wavelength of band's maximum λ_{max} and reduced band widths ($\Delta_d\tilde{\nu}$ for complexes **1**, **2**, **4**-**10** and **22**-**27**, $\Delta_d\tilde{\nu}_{blue}$ and $\Delta_d\tilde{\nu}_{red}$ for complexes **3** and **11**-**21**) defined as halfwidths of the bands after the subtraction of $\Delta\tilde{\nu}$ of anion **2**).

	HX	λ_{max} /nm	$\Delta_d\tilde{\nu}$ /cm^{-1}	$\Delta_d\tilde{\nu}_{blue}$ /cm^{-1}	$\Delta_d\tilde{\nu}_{red}$ /cm^{-1}
1	-	310.4	3340		
2	-	432.2	0		
3	2-chloro-4-nitrophenol	389.2		2650	1190
4	Hydrogen tetrafluoroborate	321.1	3060		
5	Hydrogen iodide	325.7	2990		
6	Hydrogen bromide	328.0	2930		
7	Hydrogen chloride	331.2	2800		
8	trifluoroacetic acid	336.1	2680		
9	dichloroacetic acid	340.5	2550		
10	2,3,5-trichlorobenzoic acid	344.8	2380		
11	chloroacetic acid	347.9		2450	1530
12	3,5-dichlorobenzoic acid	351.1		2410	1390
13	formic acid	358.0		2330	1240
14	4-chlorobenzoic acid	363.5		2280	1160
15	benzoic acid	374.0		2290	1090
16	4-chlorophenylacetic acid	384.0		2260	1040
17	4-tert-butylbenzoic acid	387.4		2170	1000
18	phenylacetic acid	390.9		2160	960
19	3-phenylpropionic acid	398.8		2140	890
20	acetic acid	400.2		2180	870
21	4-phenylbutyric acid	401.9		2080	820
22	pivalic acid	405.4	1090		
23	2,4,5-trichlorophenol	401.9	930		
24	4-nitrophenol				
25	2,4-dichlorophenol	405.9	810		
26	4-chlorophenol	413.6	450		
27	4-methylphenol	418.9	530		

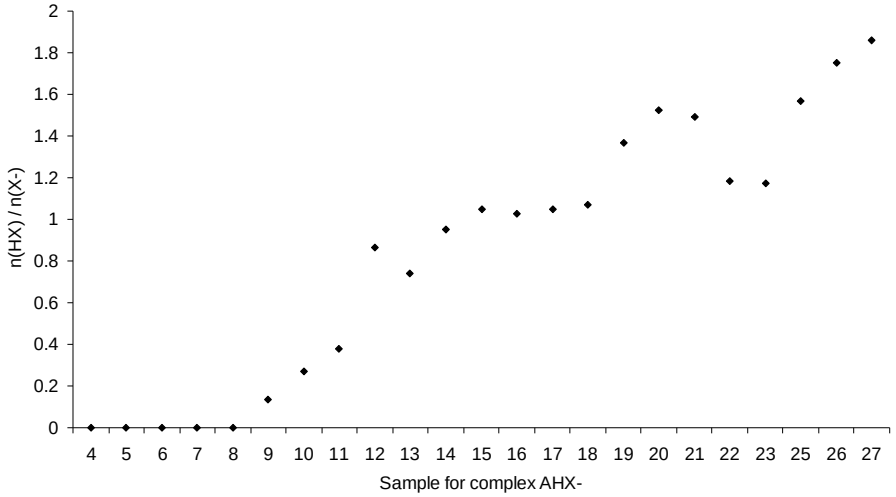

Figure S1. Ratio of n(HX)/n(X-) for UVNMR samples of complexes AHX^- calculated from values in Table S1.

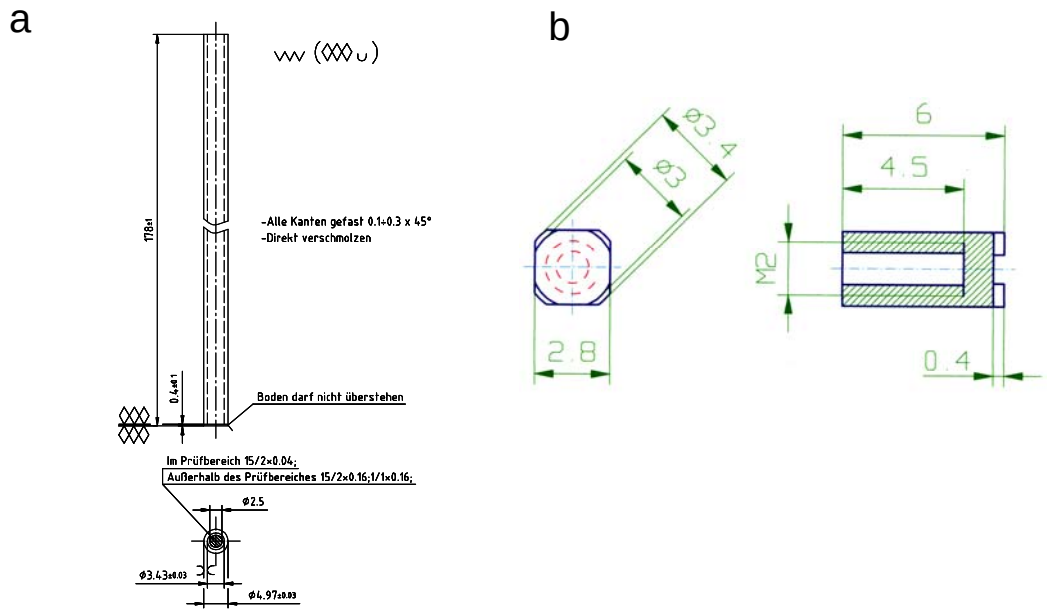

Figure S2. (a) Example of UVNMR cuvettes (drawing reproduced with kind permission from Hellma GmbH & Co. KG, Müllheim); (b) PTFE inserts for UVNMR cuvettes (drawing by Karina Hille, Freie Universität Berlin)

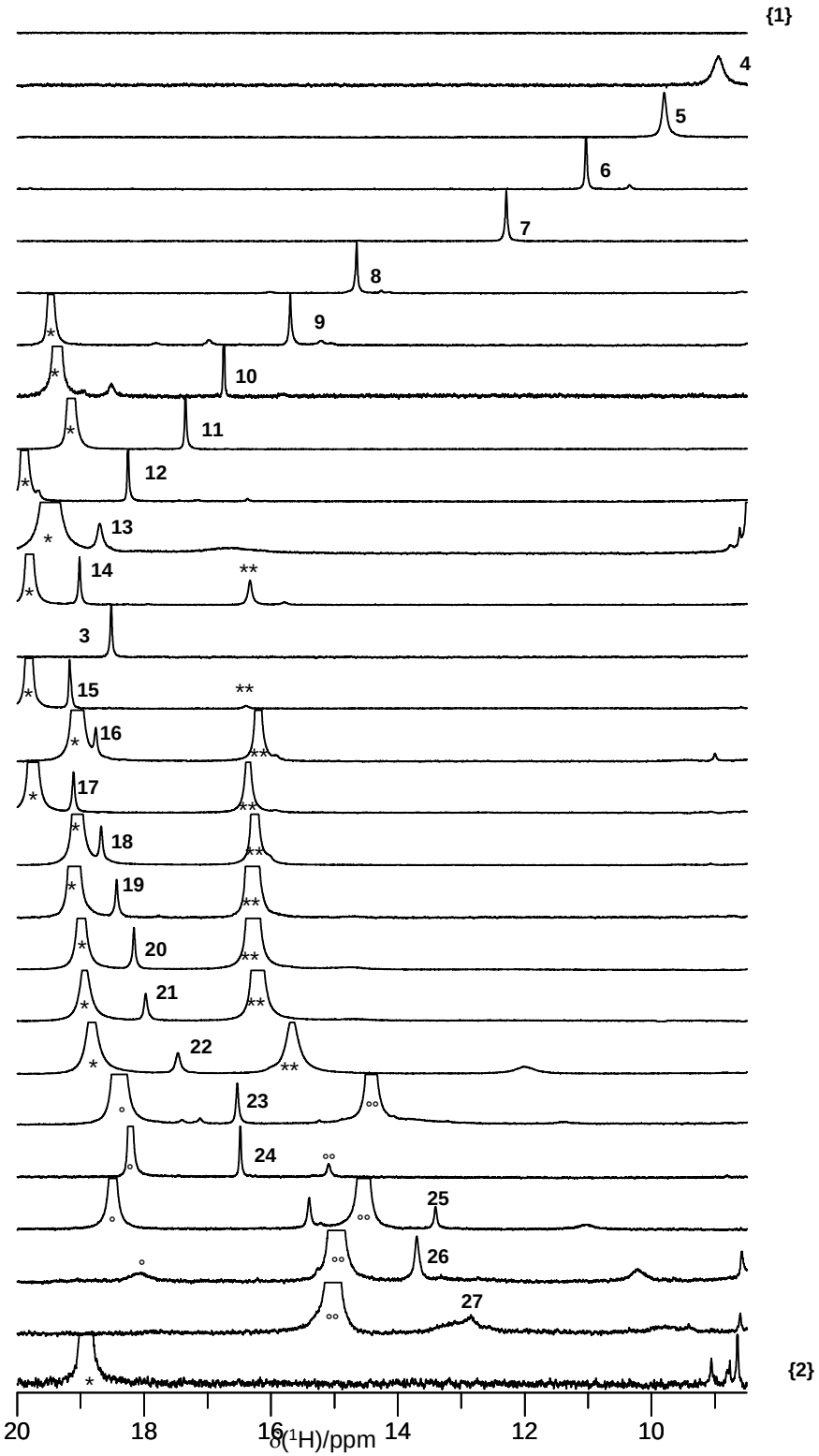

Figure S3. ^{1}H NMR spectra of UVNMR samples corresponding to ^{13}C NMR and UV/Vis spectra in Figures S4 and S5. Signals labelled with numbers correspond to bridging protons in 2-chloro-4-nitrophenol (CNP) complexes CO<u>H</u>X. Other signals are: hydrogen dicarboxylates (*) and dihydrogen tricarboxylates (**) of partner carboxylic acids HX, and hydrogen diphenolates (°) and dihydrogen triphenolates (°°) of partner phenols HX. Neutral CNP **1** does not give rise to signals in the displayed region. Aromatic protons of CNP anion **2** in the very bottom spectrum give rise to signals in the region 8-9 ppm; and the signal at 19 ppm is caused by hydrogen dipivalate stemming from the proton scavenger pivalate.

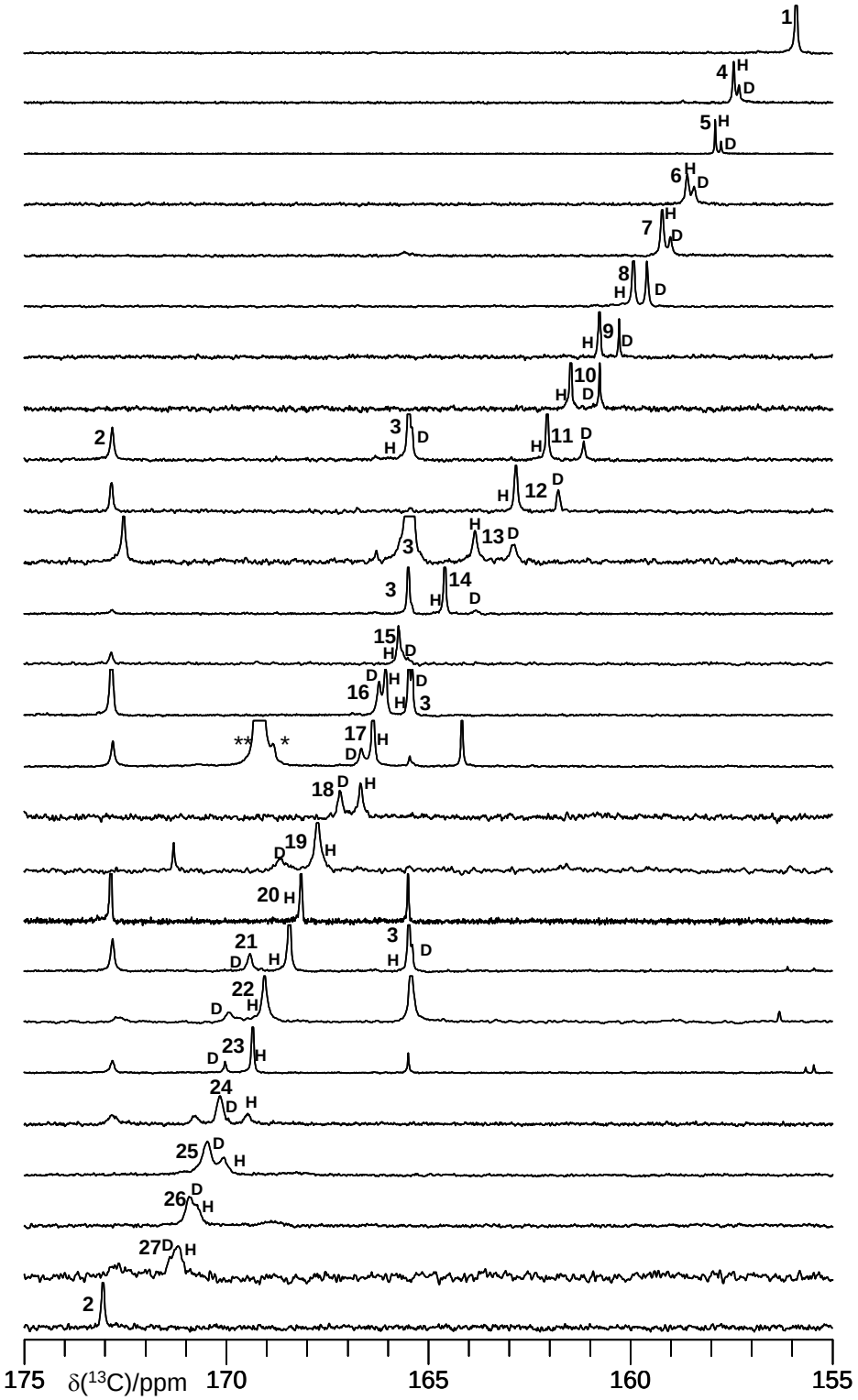

Figure S4. ^{13}C NMR spectra of partially deuterated samples from which δ(COHX) and δ(CODX) for species **1**-**27** were determined (signals are labelled with the species' numbers and H or D, resp.). Samples for species **1**, **20** and **2** were not deuterated. Some samples display signals of CNP anion **2** and CNP homo-conjugate complex **3** along with the target hetero-conjugate complex of CNP. In the sample for species **17**, the partner 4-*tert*-butylbenzoic acid was ^{13}C enriched in its carboxylic group giving rise to signals of the hydrogen dicarboxylate (*) and dihydrogen tricarboxylate (**).

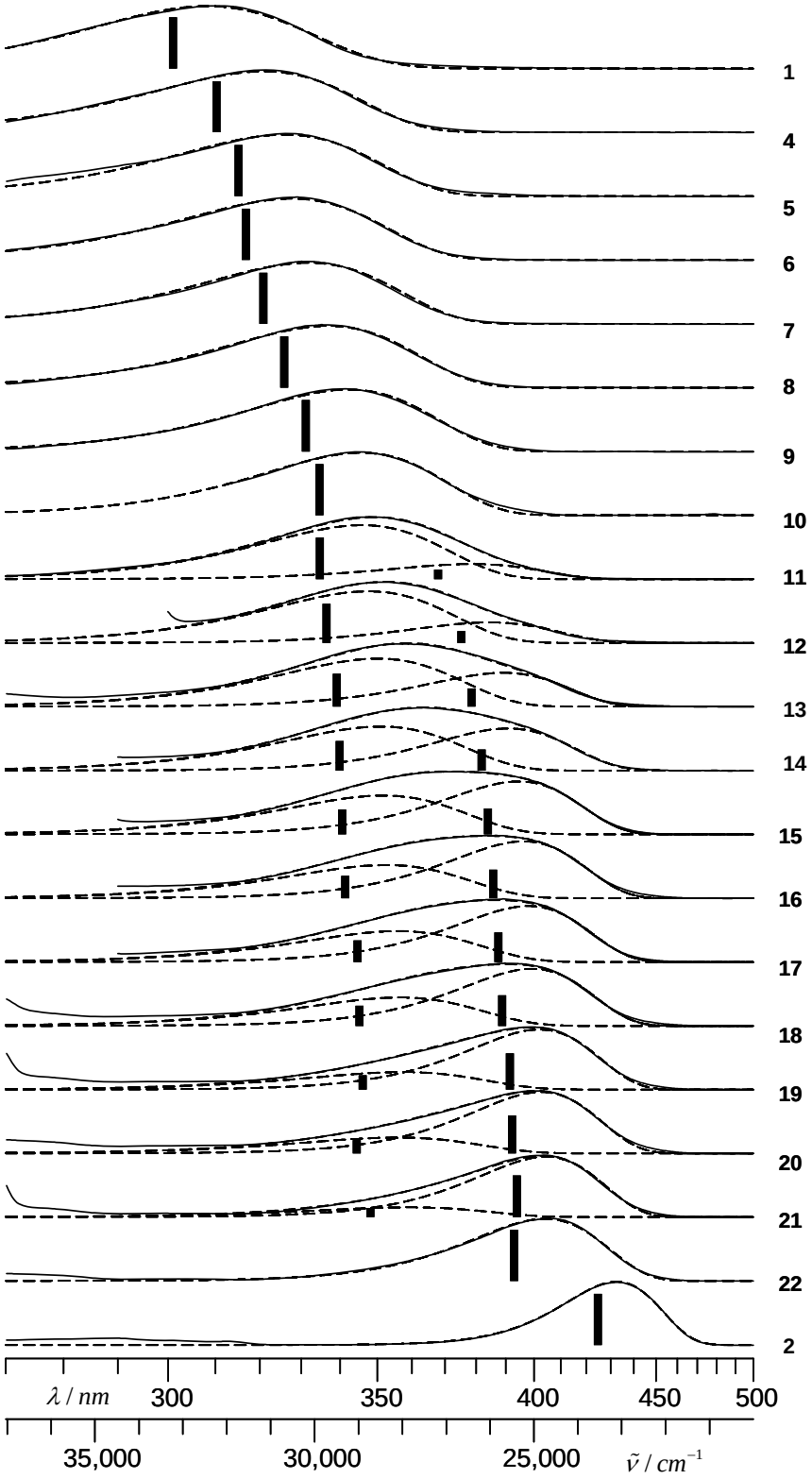

Figure S5. UV-Vis absorption spectra of neutral CNP **1**, CNP anion **2**, and hetero-conjugate complexes of CNP with acids **4**-**22**. Solid lines are experimental spectra, broken lines represent log-normal fit functions as detailed in the main text. Sticks indicate the center of gravity of each fit function and fractional integral intensities in cases **11**-**21** where there are two fit functions per spectrum. All spectra were normalized to common intensity of absorbance maxima. In spectra of **12** and **14**-**17**, the regions of strong absorbance of excess moieties of complex partners have been omitted.

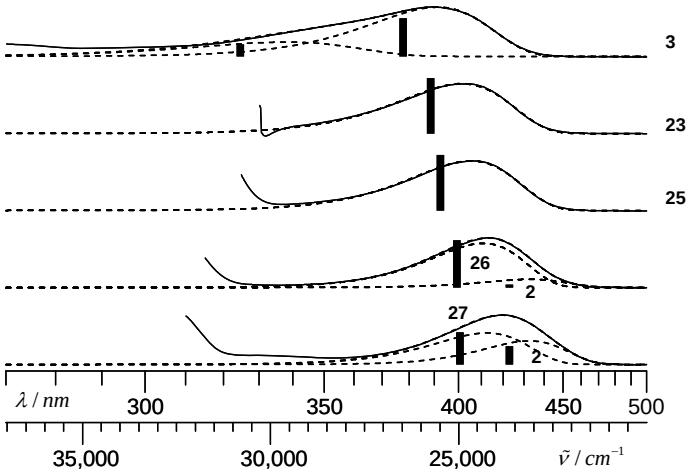

Figure S6. UV-Vis absorption spectra of CNP homo-conjugate complex **3**, and CNP hetero-conjugate complexes with other phenols **23, 25**-**27**. Conventions apply as in Figure S4.
In spectra of **23, 25**-**27** the regions of strong absorbance of excess moieties of complex partners have been omitted. Spectra of **26** and **27** were determined by measurement in the presence of **2** and subsequent deconvolution as detailed in the original text.

Chemical shift of the proton *ortho* to the hydroxyl group in CNP and hydrogen bond geometry.

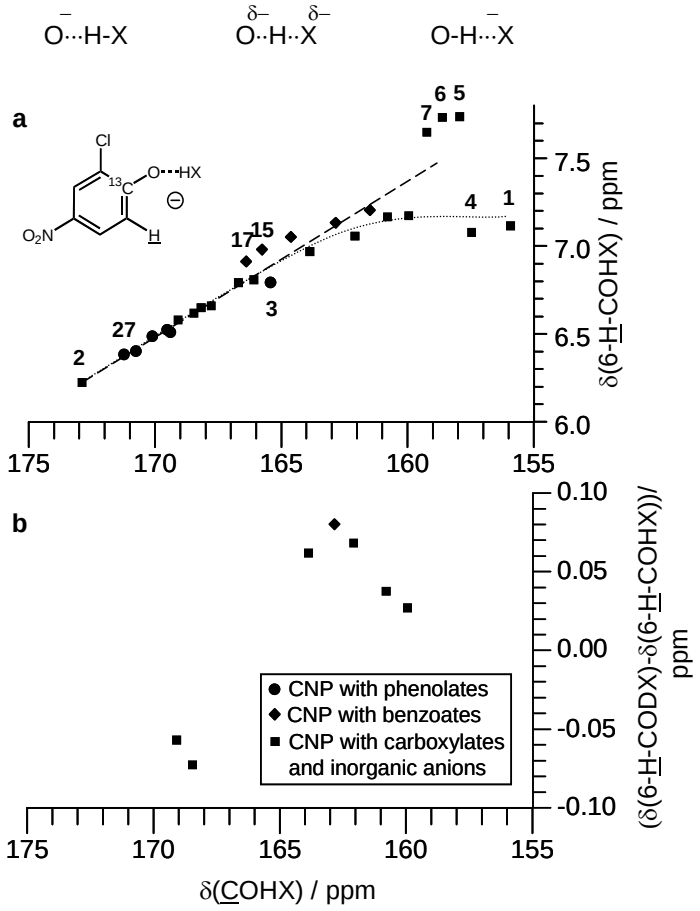

Figure S7. NMR parameters of 2-chloro-4-nitrophenol (CNP). **1**, its anion **2**, and its conjugated complex **3**-**27**. Diamonds refer to complexes where the partner to CNP is a benzoate, circles where the partner is a phenolate. In other cases the symbol is a square.
(a) Chemical shift of the proton *ortho* to the hydroxyl group, δ(6-H-COHX), plotted against the chemical shift of 1-^{13}C δ(COHX). The broken line illustrates a region of linear correlation, while the dotted line represents a proposed more general correlation.
(b) H/D isotope effects δ(6H-CODX)- δ(6H-COHX) plotted against δ(COHX).

In Figure S7a, similar to Figures 7 and 8 of the main text, distinct symbols were chosen for data relating to three groups of species to check for specific influences on spectroscopic parameters: complexes of 2-chloro-4-nitrophenolate with benzoic acids (diamonds), with phenols (circles), and the remaining cases of complexes with saturated carboxylic and inorganic acids, and the special cases of neutral **1** and non-complexed anionic **2** (squares).

Experimental parameters are correlated roughly as indicated by the dotted line (not an analytical function). In the bottom left region of the plot featuring data corresponding to anion of **2** and conjugate complexes with phenols **27** down to **23** (circles) and the next couple of data points following in the direction top right, stemming from complexes with saturated acids (rectangles) the correlation is linear and well adhered to broken line. However, starting approximately from a

carbon chemical shift of δ(COHX) =165 ppm upfield (corresponding to approx. 6.95 ppm in proton chemical shift), this linear correlation is lost and proton chemical shift is approaching a limiting value of around 7.15 ppm.

The most obvious exceptions from the proposed correlation is found in cases of complexes **5**, **6**, and **7** for which δ(6-H-COHX) is found to be 7.6-7.7 ppm. These are the three complexes of the chromophore HA with halogenide anions. Note in contrast the data of the AHX^- complex **4** with the other weak inorganic acceptor tetrafluorborate. Also note that all data points corresponding to complexes involving benzoic acids (diamonds) lie significantly above the dotted line, while all others lie on or below that line (with the only exceptions of the halogenide complexes **5**, **6**, **7** just mentioned).

We conclude that, taking into account the correlation between δ(COHX) and H-bond geometry established in the main text and the results presented in Figure S7, the *ortho* proton chemical shift δ(6-H-COHX) may be used as a measure for H-bond geometry, at least within certain limits. The correlation is fair while the chromophore (2-chloro-4-nitrophenol moiety) has substantial anionic character, but sensitivity to H-bond geometry becomes very small and other factors of the chemical environment other than hydrogen bonding at phenolic oxygen may influence the absolute chemical shift in a similar order of magnitude especially if the phenol has only little anionic character.

In this context we would like to mention that in a few cases within the series of complexes of type AHX^-, partially deuterated samples featured resolved extra signals in the ^1H NMR spectra corresponding to the *ortho* proton of the chromophore in the deuterated form of the complex (δ(6-H-CODX)). Values between -0.07 and +0.08 ppm (see Figure S7b) were observed for the secondary isotope effect δ(6-H-CODX)- δ(6-H-COHX) which is always of reversed sign compared to δ(CODX)- δ(COHX), reflecting the reverse sense of correlation between chemical shifts and protonation state.

Center of gravity absorption versus absorption maxima for usage in the characterization of convoluted bands.

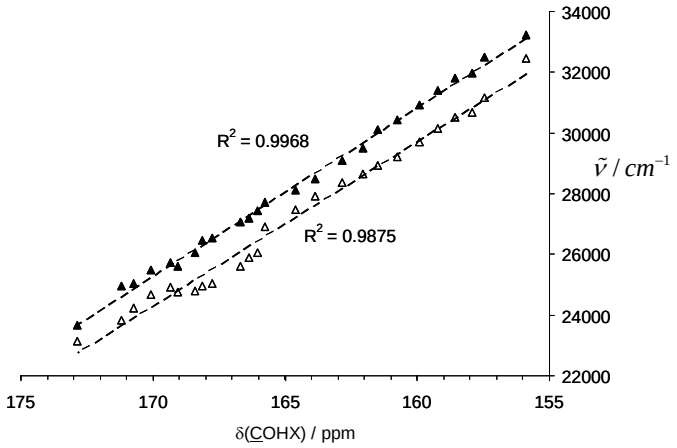

Figure S8. Positions of the UV-Vis absorption bands of the π-π* transition of the systems **1**, **2**, and **3**-**27** in CD_2Cl_2 around 175 K as a function of the chemical shift δ(COHX) of 1-^{13}C of the chromophore moiety. Centers of gravity of absorption bands are characterized by solid triangles, the positions of the absorption maxima by open triangles (in cm^{-1}).

In Figure S8, solid triangles represent the COG of absorption in wavenumber dimension $\tilde{\nu}_{COG}$ and open triangles represent the wavenumber of absorption maxima $\tilde{\nu}_{max}$ (see Table S2 for λ_{max} values, from which $\tilde{\nu}_{max}$ could be calculated). We see very good linear correlation for $\tilde{\nu}_{COG}$ and δ(COHX) and a good correlation for $\tilde{\nu}_{max}$ and δ(COHX), with slight deviations from linearity. The systematic offset is caused by the asymmetry of the bands.

The reasons why we prefer the usage of COG for the characterisation of composite bands are as follows. We remind that, as shown in the main text, δ(COHX) is a measure for the average proton position in the ensemble of complexes. By contrast, the experimental UV-Vis absorption band is a superposition of several intrinsic bands stemming from different "solvatomers" (tautomers, which differ by the structure of the solvent cage). Thus, the UV-Vis bands represent a distribution function, though potentially distorted by variations in extinction coefficients. Hence, the COG of a convoluted band again represents a (weighted) average geometry, and hence the good correlation is observed between this COG and δ(COHX).

On the other hand, the maximum of a sum of absorption bands depends in a complicated manner on shapes, relative intensities and positions of the individual bands. Moreover, a single well defined maximum is only obtained in cases of bands narrowly spaced in respect to their width. Otherwise, convoluted bands may feature broad plateaus or distinct multiple maxima. In these cases the position of the absolute maximum will not generally be a useful spectroscopic marker. In contrast, the COG remains a well defined, and potentially useful, spectroscopic marker even if applied to bands that hardly overlap.

[1]H NMR peak positions for samples Type A and Type B.

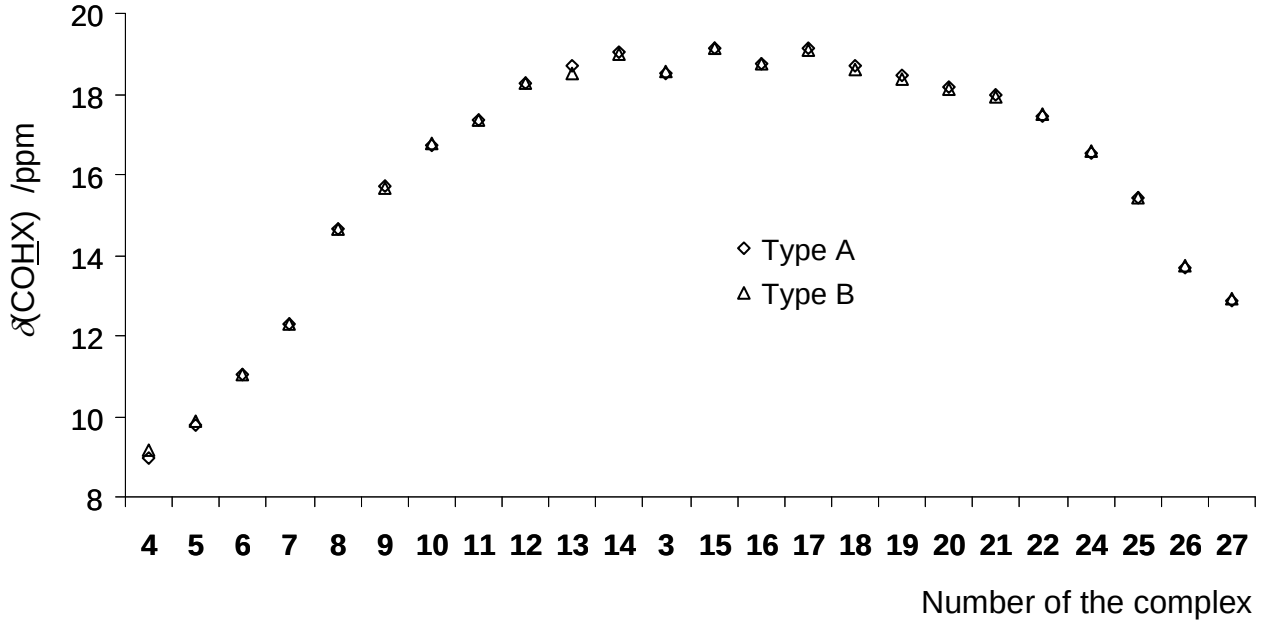

Figure S9. Comparison of the positions of the [1]H NMR signals of complexes **3**-**22** and **24**-**27** for Type A and Type B samples.